Available online at www.sciencedirect.com
SCIENCE DIRECT®
Journal of Power Sources 142 (2005) 345–353
JOURNAL OF POWER SOURCES
www.elsevier.com/locate/jpowsour

Thermal management of Li-ion battery with phase change material for electric scooters: experimental validation

Siddique A. Khateeb[a], Shabab Amiruddin[a], Mohammed Farid[b], J. Robert Selman[a], Said Al-Hallaj[a,*]

[a] *Center for Electrochemical Science and Engineering, Department of Chemical and Environmental Engineering, Illinois Institute of Technology, 10 West 33rd St., Chicago, IL 60616, USA*
[b] *Department of Chemical and Materials Engineering, University of Auckland, New Zealand*

Received 25 August 2004; accepted 17 September 2004
Available online 7 December 2004

Abstract

This work reports the laboratory test results of a Li-ion battery designed for electric scooter applications. Four different modes of heat dissipation were investigated in this experimental study: (1) natural convection cooling; (2) presence of aluminum foam heat transfer matrix; (3) use of phase change material (PCM); and (4) combination of aluminum foam and PCM. The objective of using the PCM is to lower the temperature rise of the Li-ion cells and create a uniform temperature distribution in the battery module. This is clearly justified looking at the experimental results presented in this work. The use of high thermal conductivity aluminum foam in the voids between the cells reduces the temperature rise of the Li-ion cells but is insufficient when operated in high ambient temperature such as those usually occur in summer. The use of aluminum foam with PCM causes a significant temperature drop of about 50% compared to the first case of no thermal management. It also provides uniform temperature distribution within the battery module, which is important for the efficient performance of the cells used. The laboratory results were modeled using a 2-D thermal model accounting for the four different modes of heat dissipation and good agreement was obtained between the simulation and experimental results.

Keywords: Lithium-ion battery; Thermal management; Phase change materials; Electric scooter; Thermal modeling/simulation; Air-cooling

1. Introduction

Thermal management of Li-ion batteries play a significant role in large power applications in addressing the thermal safety apart from improving the performance and extending the cycle life. The electrochemical performance of the Li-ion battery chemistry, charge acceptance, power and energy capability, cycle life and cycle life cost are very much controlled by the operating temperature [1]. One of the side effects of exposure to high temperature is fast aging and accelerated capacity fade [2]. Ramadass et al. [3] studied the capacity fade and did a complete capacity fade analysis of Sony 18650 (1.8 Ah) Li-ion cells on cycling at elevated temperatures of 45–55 °C. They elucidated that after 800 cycles, the cells lost 31% and 36% of their initial capacity at 25 °C and 45 °C, respectively. The cells cycled at 50 °C lost more than 60% of initial capacity after 600 cycles and 70% after 500 cycles at 55 °C. Therefore, maintaining an optimized and continuously regulated temperature necessitates the need for an efficient thermal management system in large Li-ion battery applications.

Proper thermal management would minimize temperature gradients between the cells in the module [4–6], which would otherwise cause a detrimental effect on the battery performance and electric vehicle sustainability. A thermal management system can completely operate as an active cooling system using air or liquid as the heat transfer medium [4,7]

* Corresponding author. Tel.: +1 312 567 3060; fax: +1 312 567 8874.
E-mail address: alhallaj@iit.edu (S. Al-Hallaj).

0378-7753/$ – see front matter © 2004 Elsevier B.V. All rights reserved.
doi:10.1016/j.jpowsour.2004.09.033

Nomenclature

Cp_{al}	specific heat capacity of aluminum foam ($kJ\,kg^{-1}\,K^{-1}$)
Cp_{cell}	specific heat capacity of Li-ion cell ($kJ\,kg^{-1}\,K^{-1}$)
Cp_{eff}	effective specific heat capacity of PCM and Al-foam ($kJ\,kg^{-1}\,K^{-1}$)
Cp_{l}	specific heat capacity of PCM in liquid phase ($kJ\,kg^{-1}\,K^{-1}$)
Cp_{s}	specific heat of PCM in solid phase ($kJ\,kg^{-1}\,K^{-1}$)
E_{eq}	equilibrium potential (V)
F	Faraday's constant (96,500 C eq^{-1})
ΔG	change of Gibbs' free energy (J)
ΔH	change of enthalpy (J)
I	current demand of Li-ion battery (A)
k_{al}	thermal conductivity of aluminum ($W\,m^{-1}\,K^{-1}$)
k_{cell}	thermal conductivity of Li-ion cell ($W\,m^{-1}\,K^{-1}$)
k_{eff}	effective thermal conductivity of PCM and aluminum foam ($W\,m^{-1}\,K^{-1}$)
k_{l}	thermal conductivity of PCM in liquid phase ($W\,m^{-1}\,K^{-1}$)
k_{s}	thermal conductivity of PCM in solid phase ($W\,m^{-1}\,K^{-1}$)
q	volumetric heat generation ($W\,cm^{-3}$)
ΔS	change of entropy ($J\,K^{-1}$)
t	time (s)
T	temperature (K)
T_{amb}	ambient temperature (K)
T_{l}	end temperature of PCM melting (K)
T_{m}	average of T_s and T_l (K)
T_{s}	start temperature of PCM melting (K)
T_{wall}	wall temperature (K)
V	voltage demand of Li-ion battery (V)
W_{el}	electric work (W)

Greek symbols

ε	porosity of a aluminum foam
λ	latent heat of melting of PCM ($kJ\,kg^{-1}$)
ρ_{al}	density of aluminum ($kg\,m^{-3}$)
ρ_{cell}	density of Li-ion cell ($kg\,m^{-3}$)
ρ_{eff}	effective density of the PCM and Al-foam ($kg\,m^{-3}$)
ρ_{l}	density of PCM in liquid phase ($kg\,m^{-3}$)
ρ_{s}	density of PCM in solid phase ($kg\,m^{-3}$)

or in a passive mode of operation without the active cooling/heating components using phase change materials (PCM) [8,9] or in a combination of these systems. An active thermal management system like air-cooling and liquid-cooling ensures thermal safety by adding accessories and complex electronics but cannot function as a stand-alone system without depending on external power. Al-Hallaj et al. [8] and Khateeb et al. [9] simulated the Li-ion battery for an electric car and a scooter with a passive thermal management system using phase change material demonstrating its feasibility. In an electric scooter application where space constraint limits the use of an active thermal management system, a passive PCM system proved to be a feasible choice.

Khateeb et al. [9] described a detailed procedure of designing Li-ion batteries for an electric scooter and presented simulation results showing the feasibility of a novel passive thermal management system for Li-ion batteries using phase change material (solid–liquid). No experimental measurements were reported in the previous publications. In this paper, the measured performance of the Li-ion battery designed for electric scooter are reported and compared with the model predictions showing good agreement.

2. Experiment design

Each Li-ion battery pack contained two modules each consisting of eighteen 18650, 2.2 Ah Li-ion cells obtained from Moli Energy, and were assembled in a 3S × 6P configuration consisting of six rows with three cells in series in each row as shown in Fig. 1. Two battery packs were assembled for independent testing of the thermal management; one using phase change material alone and the other with PCM distributed in the pores of aluminum foam. Fig. 2, shows an alternative design for the Zappy electric scooter, which was assembled in a 4S × 6P configuration where the Li-ion cells were fitted into the aluminum foam filled with PCM. This module is rated at 16 V and 13.2 Ah as compared to 12 V and 13.2 Ah for the 3S × 6P module. For testing purpose, the 3S × 6P module was tested at various C-rates with and without PCM to

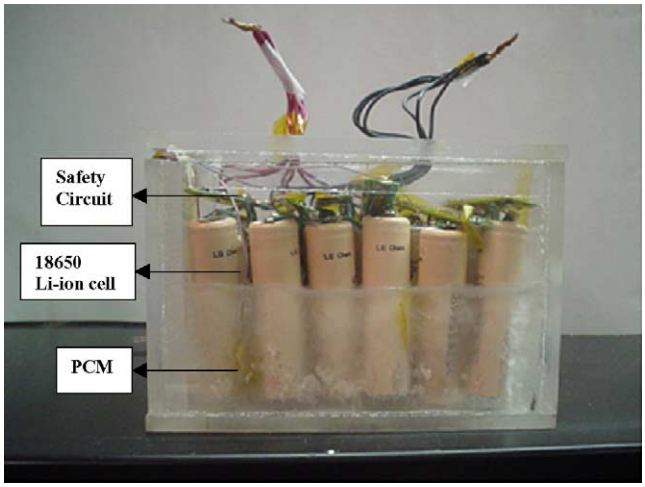

Fig. 1. Li-ion battery module filled with phase change material and connected with safety circuits.

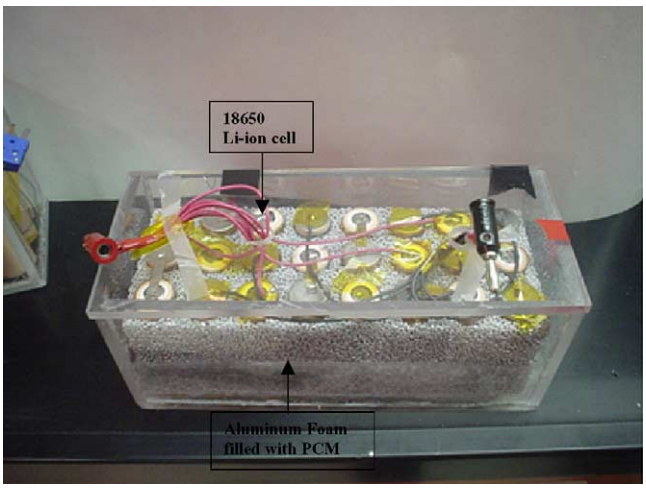

Fig. 2. Li-ion battery module surrounded by Al-foam, filled with phase change material.

measure the thermal response whereas the 4S × 6P module was tested to determine the thermal response of the aluminum foam in the absence and presence of PCM. The spacing between the cells is very critical in determining the loading factor of the phase change material inside the module. The total volume occupied by the PCM was determined from direct energy balance that allowed determining how the cells were spaced.

3. Testing protocol for the Li-ion battery modules

Two different kinds of testing protocols were employed to demonstrate the heat dissipation capability of the PCM thermal management system. This includes determining the charge/discharge capability of the Li-ion battery module—constant current characterization (CCC) testing and dynamic current characterization (DCC) testing.

3.1. Constant current characterization (CCC) test

CCC testing was performed in the laboratory using the Arbin battery cycler (Model No. BT2000, College Station, TX, USA) where the Li-ion battery module was subjected to the following charge/discharge protocol:

- *Charge period*: Galvanostatic mode at a specific *C*-rate [10] with a voltage cut-off limit of 4.2 V (12.6 V for three cells in series) followed by a potentiostatic mode until current drops to 50 mA (300 mA for six cells in parallel).
- *Rest period*: 1 h equilibration time.
- *Discharge period*: Galvanostatic mode at the same *C*-rate during the charge until the voltage drops to 3 V per cell in series (9 V for three cells in series).
- *Rest period*: 1 h equilibration time.
- *Cycle repeat*: Five cycles.

The above testing was performed at *C*/5, *C*/3, *C*/2 and *C*/1 rates representing slow to fast charge/discharge rates and for four different Li-ion battery module types: (1) cells alone; (2) cells with PCM; (3) cells with Al-foam; and (4) cells with PCM and Al-foam.

The thermal performance of the Li-ion battery module and heat dissipation effectiveness of the phase change material was evaluated from the above tests.

3.2. Dynamic current characterization (DCC) test

DCC testing determines the actual performance of the Li-ion battery module assembled into the Zappy electric scooter under different riding conditions. The original lead–acid battery of the Zappy scooter was replaced with two Li-ion battery modules with very few modifications to the scooter. The modules were connected in parallel to meet the required average current output of 24 A and 12 V nominal voltage as obtained from previous field test on lead–acid battery [9]. A portable 16-channel data acquisition system acquired from Kinetic Systems (Model No.V532, Lockport, IL, USA) was used to record the data.

4. Experimental set-up

4.1. Constant current characterization (CCC) test

The Li-ion battery module tested in the laboratory was enclosed in a cardboard box to represent the real situation when the module in placed in the Zappy scooter battery compartment. The ambient temperature varied slightly for the tests performed at different *C*-rates.

Some of the future tests are intended to test the module in a temperature chamber with different operating temperatures. The temperature was recorded using T-type thermocouples that were adhered to the Li-ion cell surface and at different location in the PCM region whenever PCM was used.

4.2. Dynamic current characterization (DCC) test

This test characterizes the performance of the Li-ion battery module in the actual riding conditions that requires real-time monitoring of the current, voltage, temperature via a portable data acquisition (DAQ) system that was mounted on the Zappy electric scooter. Due to the low current rating of the DAQ system, a shunt (75 A, 50 mV) was used to read the voltage, which was used to calculate the current. T-type thermocouples were used to record the temperature in the DAQ system.

The entire assembly of the Li-ion battery modules and the DAQ is shown in Fig. 3. The battery modules were designed to fit into the battery compartment without making any form of mechanical changes to the existing battery compartment.

Fig. 3. Assembly of two Li-ion battery modules and data acquisition (DAQ) system in Zappy electric scooter.

5. Experimental results of Li-ion battery module using battery cycler

5.1. Summary of experimental results of Li-ion (3S × 6P) battery module

For conciseness, the measured temperature rise of the Li-ion cell located at the center of the battery module and the PCM surrounding, during charge and discharge is summarized in Figs. 4 and 5, respectively. The effect of the PCM and the high thermal conductivity aluminum foam in dissipating heat is clearly observable in these figures. The cell and the PCM temperature were recorded at the center of the module.

At *C*/1 rate during charge, the temperature rise was 16 °C in the absence of PCM and aluminum foam. The only mode of heat dissipation is by natural air convection through the spaces between the cells and the battery container. On the other hand, the addition of aluminum foam brings about a 50% drop in temperature rise with a temperature gradient of

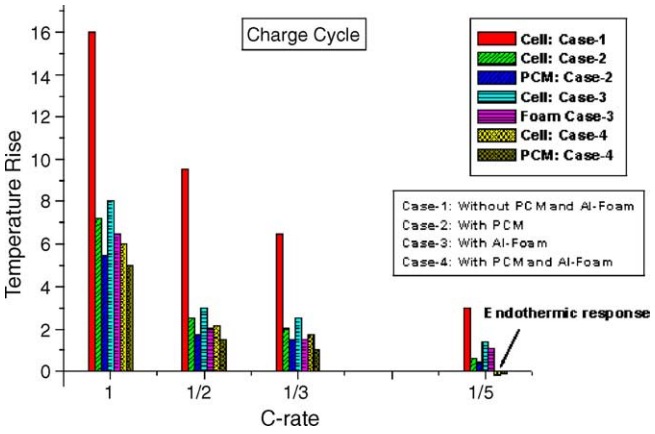

Fig. 4. Experimental results of Li-ion battery module using different heat dissipation systems during charge cycle.

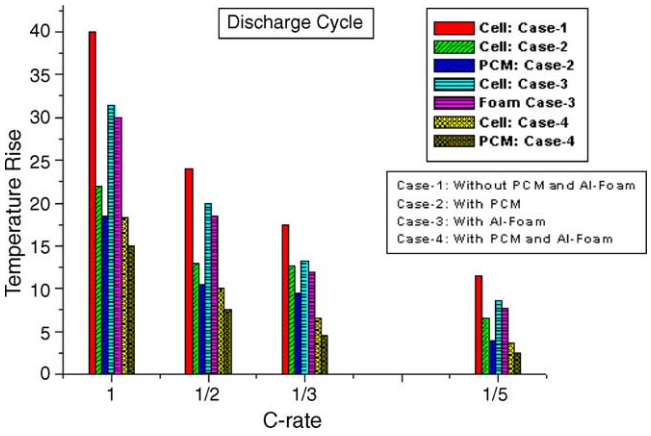

Fig. 5. Experimental results of Li-ion battery module using different heat dissipation systems during discharge cycle.

only 1 °C between the Li-ion cell and the aluminum foam. The encapsulation of the PCM in the aluminum foam causes a temperature rise of 6 °C only, which is lesser by 1–2 °C, compared to when PCM or aluminum foam were used. At other *C*-rates, there is a similar thermal behavior in all cases.

Fig. 5 represents the temperature rise of the Li-ion cell and the PCM at the center location in the Li-ion battery module during the discharge cycle at various *C*-rates for the above-explained four different cases. All these discharge tests were conducted at room temperature varying between 20 °C and 25 °C.

The *C*/1 discharge rate represents the normal maximum continuous discharge rate of the 18650 Li-ion cells as recommended by many manufacturers owing to safety reasons. Reduced discharge/charge capability at higher discharge rates and reduced cycle life are the outcome of non-regulated battery temperature that directly influences the power capability, energy storage and cycle life of the batteries [11].

For heat discharge in the absence of PCM and aluminum foam, the temperature rise of the Li-ion cell at the center of module was 40 °C. The situation can be worsened in summer with the starting temperature exceeding 40 °C; certainly natural convection cooling is not suitable under such circumstances. The addition of high thermal conductivity aluminum foam (Case 3) causes an 8 °C temperature drop as compared to the first case. But again the aluminum foam is not effective during summer operating environments. The addition of phase change material as a passive heat dissipation mechanism clearly brings about a significant drop in temperature rise of the Li-ion cell (Case 2) by almost 45% compared to the first case.

The effect of using the PCM in combination with aluminum foam (Case 4) is a decrease in temperature rise of 5 °C as compared to Case 2. The encapsulated PCM in aluminum foam can avoid any adverse thermal effects to the Li-ion battery module during summer and other harsh operating environments as was shown in a previous publication [9].

Table 1
Temperature rise of Li-ion cell at the center location during discharge using various heat dissipation mechanisms for the 3S × 6P Li-ion battery module

C-rate	Cells alone (°C)	Cells with aluminum foam (°C)	Cells with PCM (°C)	Cells with PCM and aluminum foam (°C)
C/1	42	33	26	22
C/2	25	20	13	9
C/3	18	13	10	6
C/5	12	8	7	3

At *C*/2 rate, the advantage of aluminum foam alone over the first case is not very significant with a temperature rise difference of 2.5 °C between them. The presence of PCM alone causes the temperature rise to drop by 12.5 °C as compared to Case 1 and the combination of PCM and aluminum foam causes a temperature rise of only 10 °C.

Further, as the rate of discharge is slowed, the potential of the PCM and its combination with aluminum foam does not show up a significant cut in temperature rise.

Table 1 summarizes the thermal response of the Li-ion cell at the center location in the module tested in the laboratory at various discharge rates.

The four different cases of heat dissipation mechanisms are discussed in great depth in the next section by considering only the *C*/1 rate. The experimental results are modeled and validated for the above four cases at *C*/1 rate in the following section.

6. Model development

The growing popularity of the lithium ion batteries in the last decade has attracted the researchers all over the world in developing a modeling tool to fasten the development of lithium ion batteries. Thermal modeling is an indispensable tool to study and design a thermal management system of any battery. Thermal modeling combined with electrochemical modeling of the cell produces a complete analysis, capable of predicting the thermal and electrochemical effects of the cell. The pioneering work of modeling lithium ion batteries was started by Newman and coworkers [12–14].

Assuming that the physical properties of the cell and the PCM (ρ, Cp, k) are spatially independent in the x–y region (i.e. radial direction for the cells), the energy balance equation in the cell and PCM will have the following form [12–14]:

$$\frac{\rho \mathrm{Cp} \partial T}{\partial t} = k\nabla(\nabla T) + q \tag{1}$$

The x and y derivatives only were considered in the model simulations. The volumetric heat generation term (q) is derived from fundamental thermodynamic relations as follows [15,8,16]

$$\Delta G = \Delta H - T\Delta S \tag{2}$$

$$\Delta G = -nFE_{\mathrm{eq}} \tag{3}$$

$$\Delta S = nF\frac{\mathrm{d}E_{\mathrm{eq}}}{\mathrm{d}t} \tag{4}$$

$$q = \Delta G + T\Delta S + W_{\mathrm{el}} \tag{5}$$

$$q = I(E_{\mathrm{eq}} - E) + IT\frac{\mathrm{d}E_{\mathrm{eq}}}{\mathrm{d}T} \tag{6}$$

Thus, the heat generation of the cell is a summation of irreversible heat due to the polarization effect and reversible heat terms represented by the entropic coefficient term, respectively.

The reversible and irreversible heat terms were obtained experimentally under carefully controlled experimental conditions in previous work [17]. Hence, the heat generation term used in the modeling work is an empirically derived equation at various discharge rates.

Also, the Moli (2.2 Ah) 18650 Li-ion cell used in the experimental work has higher energy capacity as compared to cells that were used in the previous work for heat generation measurements [17]. Hence, the heat generation term used in the model was scaled up proportionately.

In the phase change material region:

$q = 0$ (no heat generation)

In the phase change material region, the thermophysical properties k, ρ, Cp in Eq. (3) depends on the phase of the PCM.

The variation of the heat capacity (Cp) in the different phases of the PCM is described by the following equations [18]:

$$\mathrm{Cp} = \mathrm{Cp_s}, \quad \text{if } T \le T_{\mathrm{s}} \quad \text{(Solid Phase)} \tag{7}$$

$$\mathrm{Cp} = \mathrm{Cp_s} + \frac{\lambda(T - T_{\mathrm{s}})}{(T_{\mathrm{m}} - T_{\mathrm{s}})^2}, \quad \text{if } T_{\mathrm{s}} < T < T_{\mathrm{m}} \quad \text{(Mushy Phase)} \tag{8}$$

$$\mathrm{Cp} = \mathrm{Cp_s} + \frac{\lambda(2T_{\mathrm{m}} - T - T_{\mathrm{s}})}{(T_{\mathrm{m}} - T_{\mathrm{s}})^2}, \quad \text{if } T_{\mathrm{m}} < T < T_{\mathrm{l}} \quad \text{(Mushy Phase)} \tag{9}$$

$$\mathrm{Cp} = \mathrm{Cp_l}, \quad \text{if } T > T_{\mathrm{l}} \tag{10}$$

The thermal conductivity and density in the Mushy Phase are defined as follows:

$$k = \frac{k_{\mathrm{s}} + k_{\mathrm{l}}}{2} \tag{11}$$

$$\rho = \frac{\rho_{\mathrm{s}} + \rho_{\mathrm{l}}}{2} \tag{12}$$

The combination of PCM and aluminum foam was modeled using the following equations to define the properties of the PCM/aluminum matrix. The aluminum foam porosity (ε) is used to calculate the effective properties as follows.

Effective specific heat of PCM and Al-foam ($\mathrm{Cp_{eff}}$):

$$\mathrm{Cp_{eff}} = \varepsilon \mathrm{Cp} + (1 - \varepsilon)\mathrm{Cp_{al}} \tag{13}$$

Table 2
List of values for parameters used in simulation

Parameters	Value
λ (kJ kg^{-1})	195
ρ_{al} (kg m^{-3})	2700
ρ_{cell} (kg m^{-3})	2450
ρ_s (kg m^{-3})	910
ρ_l (kg m^{-3})	822
ε	0.80
Cp_{cell} (kJ kg^{-1} K^{-1})	1.0
Cp_{al} (kJ kg^{-1} K^{-1})	0.963
Cp_l (kJ kg^{-1} K^{-1})	1.77
Cp_s (kJ kg^{-1} K^{-1})	1.77
k_{cell} (W m^{-1} K^{-1})	3
k_{al} (W m^{-1} K^{-1})	218
k_l (W m^{-1} K^{-1})	0.21
k_s (W m^{-1} K^{-1})	0.29

Effective thermal conductivity of PCM and Al-foam is given by:

$$k_{eff} = k\varepsilon + (1-\varepsilon)k_{al} \quad (14)$$

However, the effective thermal conductivity was also calculated from a model taking into account parallel and series pore connections [19,20].

Effective density of PCM and Al-foam (ρ_{eff}):

$$\rho_{eff} = \rho\varepsilon + (1-\varepsilon)\rho_{al} \quad (15)$$

PDEase (Macsyma Inc., Massachusetts, USA) a 2-D finite element analysis (FEA) software was used for the simulation. Table 2 lists the values of the parameters used in the simulation.

7. Simulation of laboratory testing results of Li-ion battery

In order to keep the discussion concise and more interesting, comparison between the experimental results and simulation results is discussed in more depth for the battery module discharged at *C*/1 rate. Owing to the safety issues, the Li-ion cells are not continuously discharged above the *C*/1 rate as per manufacturer's recommendation. Also at higher discharge rates, the cycle life is adversely affected and requires a reliable thermal management and safety circuitry system. In the following sections, the temperature rise depicted has been normalized with respect to initial ambient temperature.

Assumptions

1. The length of charge and discharge periods in the simulation was based on the theoretical *C*-rate duration.
2. Natural convection heat transfer coefficient was assumed at the module boundary as obtained from literature.
3. Natural convection effect during phase change was ignored for simplification purpose. Such effect will reduce the temperature rise so ignoring it may be considered as a safety factor.

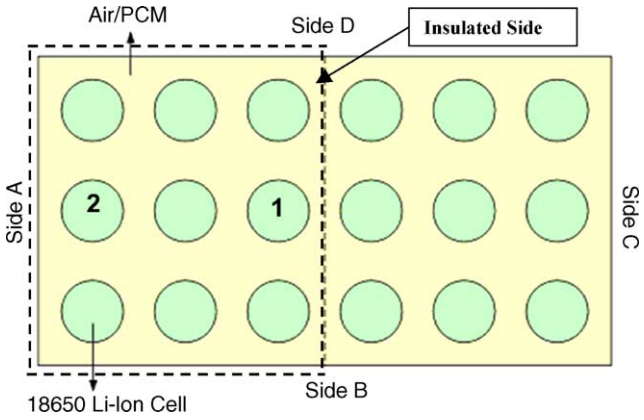

Fig. 6. Schematic of the 3S × 6P Li-ion battery module used in laboratory testing.

Fig. 6 shows the schematic of the Li-ion battery module used for laboratory testing. For simulation purpose, only the sub-module consisting of nine cells is considered due to the line of symmetry. Hence, only the left portion of the battery module in Fig. 6, represented by the dotted layout is simulated.

The boundary conditions used in the simulation are as follows:

$$\frac{dT}{dx} = \frac{dT}{dy} = 0, \quad \text{along the line of symmetry}$$

$$k\frac{dT}{dx} = -h(T_{wall} - T_{amb}),$$

at $y = 0$ on sides B, D (natural convection cooling)

$$k\frac{dT}{dy} = -h(T_{wall} - T_{amb}),$$

at $x = 0$ on sides A, C (natural convection cooling)

The value of h was assumed to be 3 W m^{-2} K^{-1} [21] between the battery wall and the ambient.

The initial ambient temperature in all the experiments was 22–25 °C.

7.1. Performance of Li-ion battery without phase change material and aluminum-foam

In Fig. 7, the experimentally measured temperature rise (line) of the Li-ion cells at two locations (1 and 2) is compared with that obtained from the simulation (line + marker) at *C*/1 charge and discharge rate for three cycles. The initial temperature was 25 °C and the temperature rise is calculated with respect to this reference temperature.

In the first charge cycle, the measured temperature rise of the Li-ion cells from the experiment is 17.5 °C as compared to 10 °C obtained from the simulation. In the following discharge cycle, the temperature rise of the Li-ion cells obtained

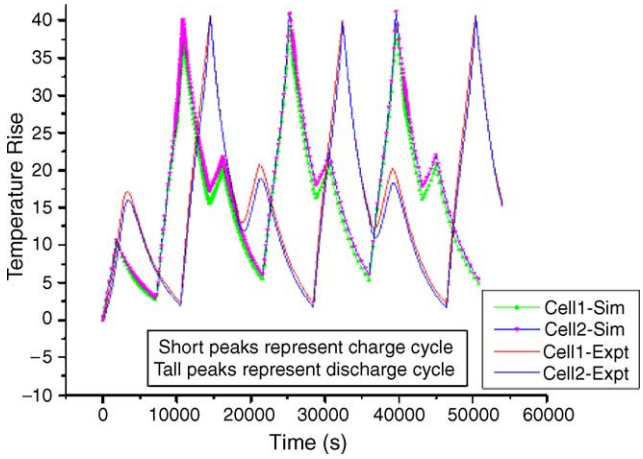

Fig. 7. Thermal response of Li-ion battery module without PCM and aluminum foam at *C*/1 rate.

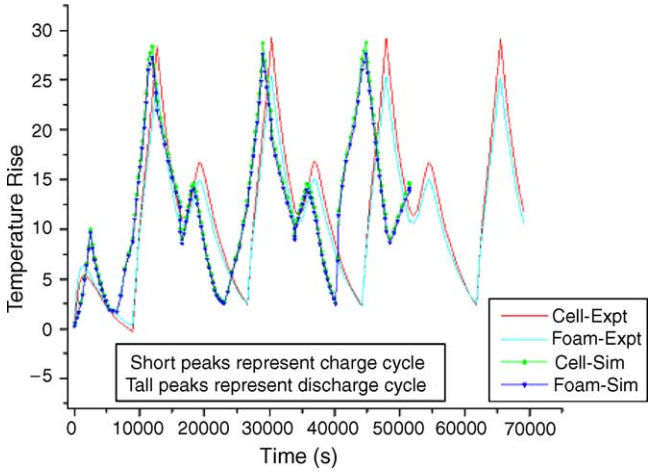

Fig. 8. Thermal response of Li-ion battery module with aluminum foam at *C*/1 rate.

from the simulation and experiment is close to 40 °C. Following the discharge, the temperature drops by 25 °C and 27 °C at the end of rest period as shown by the simulation and the experimental results respectively. In the next charge cycle, the temperature rise is 22.5 °C as predicted from the simulation and 20 °C as measured experimentally. The next consecutive charge and discharge cycle show similar response.

Though the simulation results qualitatively agree with the experimental results, the curves are shifted with respect to time scale. This is because the duration of the charge and discharge periods in the simulation was based on theoretical basis, while in real situation, the cells take longer time to charge and discharge due to growing increase in cell impedance. Also, the charging protocol in the experiment included a constant voltage step that was not accounted for in the model.

The temperature rise of 40 °C is undesirable in the Li-ion battery operation as the performance of the Li-ion cell is strongly dependent on temperature, which affects its cyclic capability and capacity retention. Thus, in the absence of any dedicated cooling or thermal management system, the temperature rises of 40 °C could affect the electrochemical performance of the Li-ion battery in the long run. Also in the case of summer operating environment, such a temperature rise can prove to be disastrous where the initial temperature can be 35–40 °C posing a risk of thermal runaway situation [22]. In the next case study, the thermal response of the Li-ion battery module is studied in the presence of aluminum foam of high thermal conductivity for quick and uniform heat dissipation.

7.2. Performance of Li-ion battery in the presence of aluminum-foam

Commercially available Duocel aluminum foam [ERG Materials and Aerospace Corporation, Oakland, CA] with a density of 8–10% and 40 ppi (pores per inch) was used for this purpose [23]. The starting temperature was close to 25 °C and the temperature rise has been normalized with respect to this temperature. Owing to the high thermal conductivity of the aluminum foam, the temperature rise of the Li-ion cell (at location 1) has dropped by 12.5 °C as compared to the previous case in the absence of aluminum foam. The temperature of the aluminum foam shown in the figure is at the adjacent location of cell 1. The temperature profiles of the Li-ion cells obtained from the simulation result agree quantitatively with the experimental results with slight variations during the charge cycles as seen in Fig. 8. Thus, a temperature rise of 27.5 °C when the ambient temperature is 40 °C put the cell close to the thermal runaway onset temperature of 70–100 °C [24]. Hence, it becomes necessary to further lower the temperature rise of the Li-ion cells for improved safety during summer.

7.3. Performance of Li-ion battery in the presence of PCM alone

The effect of utilizing phase change materials as a cost-effective thermal management solution is explored in this section. The initial temperature at the start of the experiment was 21 °C and the temperature rise has been normalized as before. With reference to Fig. 9, the temperature rise during the first charge cycle is about 8 °C for both the simulation and experimental result as compared to 17.5 °C for the experimental result in the previous case in which aluminum foam was used. In the first discharge cycle, the temperature rise of the Li-ion cell (at location 1) is 23 °C and 25 °C for the simulation and experimental results respectively as compared to 40 °C in the absence of the PCM. The PCM starts melting at 41 °C, thus leveling off the peak during its melting range of 41–44 °C as seen from the simulation and experimental result.

During the rest period following discharge, the temperature of the Li-ion cell and the PCM (adjacent to cell 1) drops by 6 °C. It is very important that the PCM solidifies after the discharge period so that the latent heat can be utilized in the

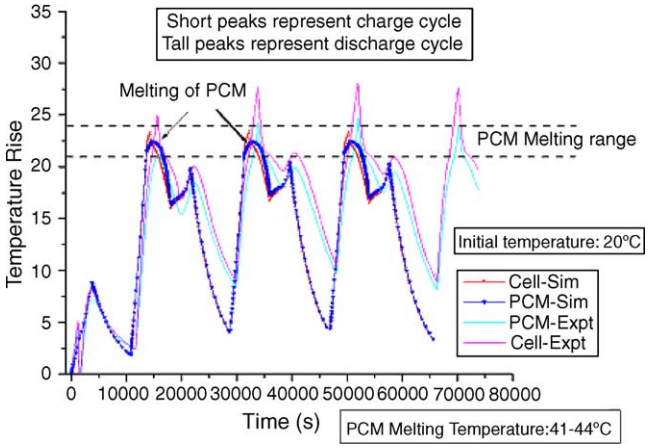

Fig. 9. Thermal response of Li-ion battery module with PCM at *C*/1 rate.

next discharge cycle. In the second charge cycle, the temperature rise remains the same as shown by the experimental and simulation results. During the rest period following this charge cycle, the Li-ion cell and the PCM cool down fast to 15 °C as predicted by the model. The measured temperature drop was only10 °C, probably due to the high heat transfer coefficient assumed in the simulation. The effect of the PCM is clearly demonstrated in this case where the temperature rise of the Li-ion cells has dropped by 15 °C by utilizing the latent heat of the PCM when compared to first case without aluminum foam and PCM as described above.

7.4. Performance of Li-ion battery with phase change material (PCM) distributed in aluminum foam

The effect of the distribution of the phase change material in the pores of the aluminum foam is studied in this case at *C*/1 charge and discharge rate. The initial ambient temperature was 19 °C and the temperature profile was normalized to this temperature. The experimental and simulation results are shown in Fig. 10. The temperature rise of the Li-ion cells has dropped by 17.5 °C when compared to the first case in the absence of aluminum foam and PCM. The thermal response of the Li-ion cell and the PCM is similar to the previous case but with a further drop in the cell temperature rise of 3–5 °C during the discharge cycle.

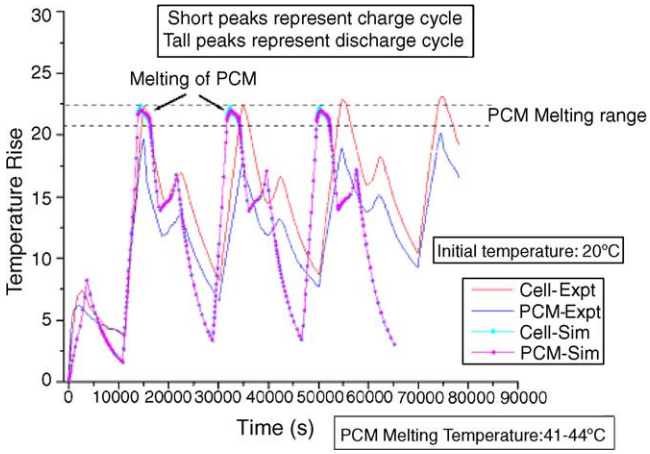

Fig. 10. Thermal response of Li-ion battery module with PCM and aluminum foam at *C*/1 rate.

It is important to note here that if PCM is used alone and in the presence of excessive heat accumulation in the battery, the PCM may melt completely and will not be able anymore to absorb the generated heat. Such condition, which may lead to battery thermal runaway could be prevented by using aluminum foam with the PCM.

8. Conclusions

The Li-ion battery module assembled as specified for the scooter was tested in the laboratory at various *C*-rates. The objective was to observe the effects of four different heat dissipation modes during charge and discharge cycling as discussed below:

(1) In the absence of aluminum foam and PCM, the module showed significant temperature rise during charge and discharge at all *C*-rates. This clearly supports the objective of using thermal management system in Li-ion battery applications; otherwise the battery will be prone to reach thermal runaway, especially in summer and harsh operating environments.
(2) Surrounding the Li-ion cells by an aluminum foam heat conductor matrix causes significant temperature drop but not enough to contain the battery in safe thermal limits during normal and abusive operating conditions.
(3) The use of PCM in gaps between Li-ion cells, resulted in a large drop in temperature rise. But the poor thermal conductivity of PCM can result in slow heat dissipation to the surrounding which leads to complete melting of the PCM during abusive battery operation, thus creating unfavorable thermal environment for the battery.
(4) The distribution of PCM in the pores of aluminum foam heat conductor resulted in a minor temperature drop when compared to PCM alone, but could be effective and necessary, under hot summer condition and other harsh thermal conditions.

A good qualitative agreement was obtained between experimental and simulation results. Future work requires a series of measurements to investigate the effect of heat conductor and PCM under high-temperature ambient condition close to the melting point of the PCM used. The suitability of a variety of PCMs with different melting ranges is of special interest under these conditions.

Acknowledgements

The authors are grateful for the financial support provided by All Cell Technologies, LLC (Chicago, IL) and the ITEC

group (Chicago, IL). Technical support by MicroSun Technologies is also acknowledged.

References

[1] A. Pesaran, J. Power Sources 110 (2) (2002) 377–382.
[2] R.B. Wright, J.P. Christophersen, C.G. Motloch, J.R. Belt, C.D. Ho, V.S. Battaglia, J.A. Barnes, T.Q. Duong, R.A. Sutula, J. Power Sources 119–121 (2003) 865–869.
[3] P. Ramadass, B. Haran, R. White, B.N. Popov, J. Power Sources 112 (2002) 614–620.
[4] A. Pesaran, First Annual Advanced Automobile Battery Conference, February 2001, http://www.ctts.nrel.gov/BTM/fctsht.html#2001.
[5] D.Y. Jung, B.H. Lee, S.W. Kim, J. Power Sources 109 (2002) 1–10.
[6] P. Arora, R.E. White, M. Doyle, J. Electrochem. Soc. 145 (10) (1998) 3647–3667.
[7] P. Nelson, D. Dees, K. Amine, G.L. Henriksen, J. Power Sources 110 (2002) 349–356.
[8] S. Al-Hallaj, J.R. Selman, J. Electrochem. Soc. 147 (9) (2000) 3231–3236.
[9] S.A. Khateeb, M.M. Farid, J.R. Selman, S. Al-Hallaj, J. Power Sources 128 (2004) 292–307.
[10] I. Buchmann, Batteries in Portable World (Chapter 5), http://www.buchmann.ca/chap5-page1.asp.
[11] A. Pesaran, J. Power Sources 110 (2002) 377–382.
[12] M. Doyle, T.F. Fuller, J. Newman, J. Electrochem. Soc. 140 (6) (1993) 1526–1533.
[13] C.R. Pals, J. Newman, J. Electrochem. Soc. 142 (10) (1997) 3274–3281.
[14] L. Rao, J. Newman, J. Electrochem. Soc. 144 (8) (1997) 2697–2704.
[15] S. Al-Hallaj, H.M. Maleki, J.S. Hong, J.R. Selman, J. Power Sources 83 (1999) 1–8.
[16] K. Onda, H. Kameyama, T. Hanamoto, K. Ito, J. Electrochem. Soc. 150 (3) (2003) A285–A291.
[17] J.S. Hong, H. Maleki, S. Al-Hallaj, L. Redey, J.R. Selman, J. Electrochem. Soc. 145 (5) (1998) 1489–1501.
[18] M.M. Farid, F.A. Hamad, M.A. Arabi, Energy Convers. Manage. 39 (8) (1998) 809–818.
[19] K. Boomsma, D. Poulikakos, F. Zwick, Mech. Mater. 35 (2003) 1161–1176.
[20] A. Sullins, K. Daryabeigi, American Institute of Aeronautics and Astronautics, AIAA 2001–2819, 35th AIAA Thermophysics Conference, 2001.
[21] J.P. Holman, Heat Transfer, eighth ed., McGraw-Hill Publisher, New Jersey, 2002.
[22] A.M. Andersson, K. Edstrom, J.O. Thomas, J. Power Sources 81–82 (1999) 8–12.
[23] ERG Materials and Aerospace Corporation (900 Stanford Ave, Oakland, CA) Technical Manual, http://www.ergaerospace.com/.
[24] A.M. Andersson, K. Edstrom, J.O. Thomas, J. Power Sources 81–82 (1999) 8–12.